

# 1-[3-Aminobenzisoxazol-5'-yl]-3-trifluoromethyl-6-[2'-(3-(*R*)-hydroxy-*N*-pyrrolidinyl)methyl-[1,1']-biphen-4-yl]-1,4,5,6-tetrahydropyrazolo-[3,4-*c*]-pyridin-7-one (BMS-740808) a highly potent, selective, efficacious, and orally bioavailable inhibitor of blood coagulation factor Xa

Donald J. P. Pinto,<sup>a,\*</sup> Michael J. Orwat,<sup>a</sup> Mimi L. Quan,<sup>a</sup> Qi Han,<sup>c</sup> Robert A. Galembo, Jr.,<sup>f</sup> Eugene Amparo,<sup>a</sup> Brian Wells,<sup>g</sup> Christopher Ellis,<sup>j</sup> Ming Y. He,<sup>k</sup> Richard S. Alexander,<sup>f</sup> Karen A. Rossi,<sup>c</sup> Angela Smallwood,<sup>i</sup> Pancras C. Wong,<sup>b</sup> Joseph M. Luetgen,<sup>b</sup> Alan R. Rendina,<sup>b</sup> Robert M. Knabb,<sup>b</sup> Lawrence Mersinger,<sup>g</sup> Charles Kettner,<sup>a</sup> Steven Bai,<sup>h</sup> Kan He,<sup>d</sup> Ruth R. Wexler<sup>a</sup> and Patrick Y. S. Lam<sup>a</sup>

<sup>a</sup>Discovery Chemistry Bristol-Myers Squibb Pharmaceutical Research Institute, Princeton, NJ 08543, USA

<sup>b</sup>Discovery Biology Bristol-Myers Squibb Pharmaceutical Research Institute, Princeton, NJ 08543, USA

<sup>c</sup>CADD Bristol-Myers Squibb Pharmaceutical Research Institute, Princeton, NJ 08543, USA

<sup>d</sup>PCO-MAP Bristol-Myers Squibb Pharmaceutical Research Institute, Princeton, NJ 08543, USA

<sup>e</sup>Incyte Corporation, Wilmington, DE 19880, USA

<sup>f</sup>Johnson & Johnson, Pharmaceutical Research and Development, Extol, PA 19341, USA

<sup>g</sup>E.I. DuPont Central Research and Development, Wilmington, DE 19880, USA

<sup>h</sup>Centocor, Malvern, PA 19355, USA

<sup>i</sup>GlaxoSmithKline, King of Prussia, PA 19406, USA

<sup>j</sup>Proctor & Gamble Pharmaceuticals, Mason, OH 45040, USA

<sup>k</sup>PfizerGlobal R&D, LaJolla, CA 92121, USA

Received 4 January 2006; revised 15 February 2006; accepted 17 February 2006

Available online 30 May 2006

**Abstract**—Attempts to further optimize the pyrazole factor Xa inhibitors centered on masking the aryl aniline P4 moiety. Scaffold optimization resulted in the identification of a novel bicyclic pyrazolo-pyridinone scaffold which retained fXa potency. The novel bicyclic scaffold preserved all binding interactions observed with the monocyclic counterpart and importantly the carboxamido moiety was integrated within the scaffold making it less susceptible to hydrolysis. These efforts led to the identification of 1-[3-aminobenzisoxazol-5'-yl]-3-trifluoromethyl-6-[2'-(3-(*R*)-hydroxy-*N*-pyrrolidinyl)methyl-[1,1']-biphen-4-yl]-1,4,5,6-tetrahydropyrazolo-[3,4-*c*]-pyridin-7-one **6f** (BMS-740808), a highly potent (fXa  $K_i$  = 30 pM) with a rapid onset of inhibition ( $2.7 \times 10^7 \text{ M}^{-1} \text{ s}^{-1}$ ) in vitro, selective (>1000-fold over other proteases), efficacious in the AVShunt thrombosis model, and orally bioavailable inhibitor of blood coagulation factor Xa.

© 2006 Elsevier Ltd. All rights reserved.

**Keywords:** Razaxaban; BMS-740808; Coagulation; Warfarin; Mutagenicity; Strategies; Clotting times; Factor Xa; Selectivity; Permeability; Pharmacokinetics; Bioavailability.

\* Corresponding author. Tel.: +1 609 818 5295; e-mail: [Donald.Pinto@bms.com](mailto:Donald.Pinto@bms.com)

Normal hemostasis is a balanced process of blood coagulation and clot dissolution. In the course of a thrombotic event, the hemostatic balance is disturbed, leading to excess clot formation which, if not treated, leads to a serious thrombotic state. Currently, the only approved oral anticoagulant in the US is warfarin sodium (Coumadin®).<sup>1a,b,c</sup> Other parenteral treatments such

as heparin, low molecular weight heparins (LMWH), and fondaparinux are also available for the prevention and treatment of thromboembolic diseases.<sup>2,3,4a–c</sup> The coagulation cascade provides many opportunities for anticoagulant intervention. Factor Xa (fXa), a key enzyme in this cascade, is a trypsin-like serine protease which catalyzes the conversion of prothrombin to thrombin, the final enzyme that triggers clot formation.<sup>5a–g</sup> Several pre-clinical animal models have suggested that targeting the fXa mechanism has the potential of providing good antithrombotic efficacy with minimal risk of bleeding.<sup>5f,g</sup> Recently, we described our efforts which led to the identification of razaxaban (BMS-561389), a potent factor Xa inhibitor with good efficacy and minimal bleeding in animals and humans.<sup>6a,b,c</sup> Razaxaban, a pyrazole based fXa inhibitor, is both potent and selective (fXa  $K_i$  = 0.19 nM, trypsin  $K_i$  > 10,000 nM) and has good oral bioavailability. The improved selectivity profile of razaxaban, relative to earlier candidates such as DPC423 (fXa  $K_i$  = 0.13 nM, trypsin  $K_i$  = 60 nM),<sup>7</sup> and DPC602 (fXa  $K_i$  = 0.91 nM, trypsin  $K_i$  = 3500 nM)<sup>8</sup> (Fig. 1), is the result of employing the larger SI specificity pocket in factor Xa (Ala 190 in factor Xa compared to Ser190 in trypsin).<sup>9</sup> A common feature in razaxaban, DPC423, and DPC602 is the presence of the 5-pyrazolo-carboxamido linker. As part of our optimization strategy, we sought to modify the carboxamido portion of the molecule to make it less susceptible to potential in vivo hydrolysis, as we were keenly aware that metabolic hydrolysis of this linker could potentially result in biarylamine fragments which could be mutagenic.

The bicyclic pyrazolo-dihydropyridinone scaffold was prepared according to the methodology outlined in Scheme 1. The starting material **1** was readily prepared in excellent yield (80–90%) following a two-step sequence from either 4-iodoaniline (R = H) or 2-fluoro-4-iodoaniline (R = F) and 5-bromovaleryl chloride (10% NaOH and DCM) followed by treatment with potassium *tert*-butoxide. Chlorination of **1** with phos-

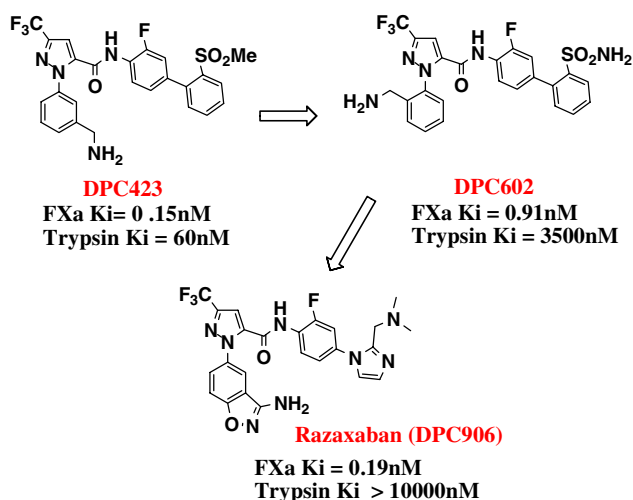
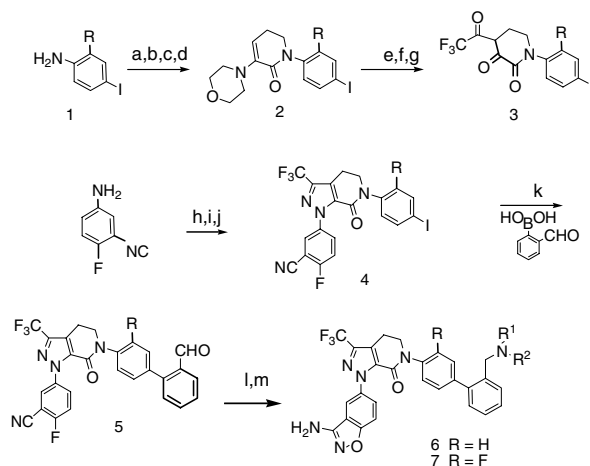


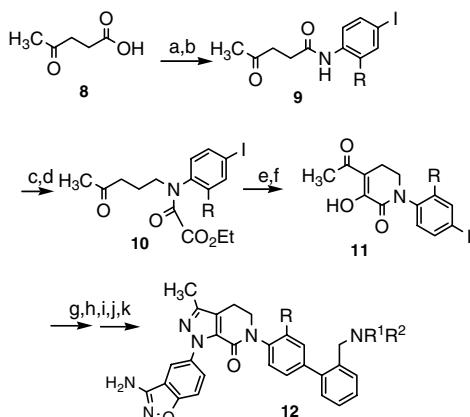
Figure 1. Pyrazole fXa inhibitors.



**Scheme 1.** General method of synthesis of the 3-trifluoromethylpyrazolo-pyridinone factor Xa compounds. Reagents and conditions: (a) 5-Br-valeryl chloride, NaOH (10%) THF; (b) 2 equiv KO<sup>t</sup>Bu; (c) PCl<sub>5</sub> (3 equiv), CHCl<sub>3</sub>; (d) morpholine excess 140 °C; (e) DMAP/TFAA/DCM; (f) Et<sub>2</sub>O, 20% aq HCl; (g) HCl, H<sub>2</sub>O; (h) NaNO<sub>2</sub>, HCl, AcOH; (i) SnCl<sub>2</sub>, H<sub>2</sub>O, HCl; (j) **3**, MeOH; (k) (Ph<sub>3</sub>P)<sub>4</sub>Pd, K<sub>3</sub>PO<sub>4</sub>, dioxane; (l) 3-OH-pyrrolidine (2 equiv), NaCNBH<sub>3</sub>; (m) Ac-NHOH, K<sub>2</sub>CO<sub>3</sub>, DMF.

phorus pentachloride, in refluxing chloroform, afforded the  $\alpha\alpha$ -dichloro-piperidinone intermediate, which on heating to reflux with excess morpholine provided the morpholine-enamine **2** in about 70% yield. Treatment of enamine **2** with trifluoroacetic anhydride in the presence of DMAP, followed by acid hydrolysis, afforded the trifluoroacetyl-piperidine-2,3-dione intermediate **3** in high yield (>90%). Condensation of **3** with 3-cyano-4-fluorophenylhydrazine afforded the required bicyclic pyrazole scaffold intermediate **4** in moderate yield (40–50%). Palladium-catalyzed Suzuki cross-coupling of the iodo intermediate **4** with 2-formylphenylboronic acid afforded the biarylaldehyde intermediate **5** (85% yield). Reductive amination of **5** with various amines provided the biarylaminomethyl P4 intermediates which on further treatment with acetohydroxamic acid and potassium carbonate in DMF<sup>9</sup> afforded the desired aminobenzisoxazole compounds **6** (R = H) or **7** (R = F) in moderate yields (40–50% yield for the two steps). The bicyclic pyrazolo-azepinone scaffold analogs were also constructed in a similar manner. The synthesis of the pyrazolo-pyrimidinone compounds was accomplished according to the methodology described by Ref. 10.

The synthesis of the 3-methylpyrazolo-pyridinone compounds is shown in Scheme 2. Coupling of 3-oxopentanoic acid **8** with the requisite aniline via oxalyl chloride and DMF afforded the keto-amido intermediate **9** in quantitative yield. This intermediate was further reduced (LAH/THF), acylated (ethylloxalylchloride/dichloromethane), oxidized (Swern) and cyclized (sodium methoxide in methanol) to afford the key lactam-dione intermediate **11** in approximately 40% yield. Condensation of **11** with 4-fluoro-3-cyanophenylhydrazine followed by the sequence of reactions described in Scheme 1 afforded the desired 3-methylpyrazolo-tetrahydropyridinone compounds **12**.



**Scheme 2.** Synthesis of the 3-methylpyrazolo-pyridinone factor Xa compounds. Reagents and condition: (a)  $(\text{COCl})_2$ ,  $\text{CHCl}_3$ ; (b) DMAP, 4-iodo-aniline,  $\text{CHCl}_3$ ; (c) LAH, THF; (d) ethyl oxalyl chloride, TEA, THF; (e) Swern; (f) NaOMe, MeOH reflux; (g) 3-CN-4-F-aniline,  $\text{NaNO}_2$ , HCl, AcOH; (h)  $\text{SnCl}_2$ ,  $\text{H}_2\text{O}$ , HCl; (i) **3**, MeOH,  $(\text{Ph}_3\text{P})_4\text{Pd}$ ,  $\text{K}_3\text{PO}_4$ , dioxane; (j) 3-OH-pyrrolidine (2 equiv),  $\text{NaCNBH}_3$ ; (k) AcNHOH,  $\text{K}_2\text{CO}_3$ , DMF.

With the discovery of razaxaban, our next focus was to identify suitable candidates that lacked the potential issue of an aniline P4. There is precedent in the literature for mutagenicity with some biarylanilines.<sup>18</sup> Moreover, the biaryl fragment of DPC602 tested positive in the Ames assay and was confirmed to be positive in the follow-up assays for mutagenicity. On the other hand, it was gratifying to determine that the aminomethyl imidazole-aniline P4 moiety of razaxaban tested negative in the Ames assay. Several additional diverse aminobiaryls and aminophenylimidazole found in our fXa inhibitors were evaluated without a clear SAR (i.e., many were not mutagenic but closely related compounds were). With this set of data in hand, it became clear that advancement of additional molecules from the monocyclic pyrazole series would require tedious investigations into the hydrolysis of the carboxamido linker and test each aminophenyl P4 in the Ames assay. To circumvent this, three strategies (Fig. 2) were employed in an effort to prevent cleavage of the carboxamido linker to the corresponding aminobiaryls.

Herein, we wish to report on the progress made with strategy I. The other approaches (strategies II and III) will be discussed in subsequent publications.<sup>10</sup> In strategy I, the potential in vivo cleavage of the carboxamido linker is prevented by its cyclization to the pyrazole scaffold. Table 1 depicts some of the pyrazolo bicyclic scaffolds which were investigated. In general, these scaffolds maintained the subnanomolar inhibitory activity against factor Xa, previously observed with razaxaban and the monocyclic pyrazole prototype **15**.<sup>19</sup> In fact, **6a** was the most potent compound with a fivefold enhancement in potency relative to razaxaban. While these results were gratifying, some minor SAR differences did emerge with this study. For example, in the series lacking the tied-back ring, the *ortho*-fluoro P4 substituent added potency, however, the *ortho*-fluoro P4 substituted in the biaryl compound **7a** was comparatively less potent to the corresponding unsubstituted analog **6a**. The scaffold size clearly

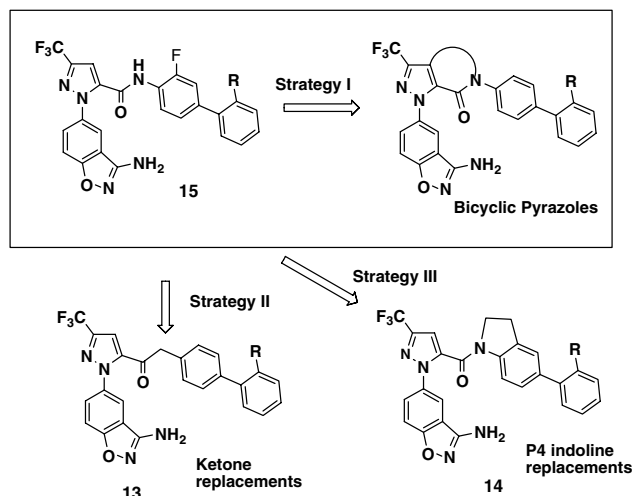


**Figure 2.** Pyrazole optimization strategies.

impacted the fXa potency. For example, compounds **6a** and **7a** were more potent when compared to the azepinone compounds **16a,b**. Introduction of a double bond in the azepinone ring showed no difference in potency (**17a,b** compared to **16a,b**). Despite the sub-nanomolar binding affinity of these analogs, these compounds exhibited weaker activity in the in vitro clotting assays than expected based on their potencies in the binding assays. To try to address these weak clotting time values, we investigated pyrazole bicyclic pyrimidinone compound **18**.<sup>10</sup> Although the potency of the pyrimidinone compound **18** in the binding assay was reduced relative to the pyrazolo-dihydropyridinone compound **6a**, an improvement was indeed observed in the clotting (PT) values. Additional information on the pyrazolo-pyrimidinyl bicyclic scaffold will be the subject of discussion in future communications.<sup>10</sup>

The effect of modifications on the biaryl moiety is illustrated in Table 2. In general, most of the compounds show potent inhibition of fXa. The SAR clearly shows a preference for a diamino-substitution on the biaryl moiety. For example, compound **6a** (fXa  $K_i = 0.04$  nM) and compound **6b** (fXa  $K_i = 0.11$  nM) compared to compound **6d** (fXa  $K_i = 0.34$  nM). The potency was enhanced when one of the ethyl groups of **6b** was replaced with a methyl group (**6c**, fXa  $K_i < 0.10$  nM). Pyrrolidine **6e** was potent against fXa ( $K_i = 0.15$  nM), however, a significant enhancement in potency was seen by the introduction of a 3(*R*)-hydroxyl moiety on the pyrrolidine ring (e.g., **6f** fXa  $K_i = 0.03$  nM). The 3(*S*)-pyrrolidine isomer **6g** (fXa  $K_i = 0.12$  nM) was about fourfold less potent. Between the two compounds, **6f** showed the best balance of potency in the binding assay and in the in vitro clotting assay. The morpholine and piperazine containing compounds **6i–k** were potent fXa inhibitors, but were weaker in the clotting assay. In general, the compounds in this series were highly selective relative to trypsin ( $K_i > 10,000$ ), but showed reduced selectivity for thrombin. Compound **6f** showed the highest affinity for thrombin ( $K_i = 35$  nM). As previously described, the pyrazolo bicyclic compounds lacking the 2'-fluorobiaryl substituent are more potent in

**Table 1.** In vitro activity for various bicyclic pyrazole scaffolds

Compound	Scaffold	R	fXa $K_i$ (nM)	PT $EC_{2x}$ ( $\mu$ M)
<b>6a</b>		H	0.04	2.7
<b>7a</b>		F	0.13	5.6
<b>16a</b>		H	0.81	4.0
<b>16b</b>		F	0.85	8.5
<b>17a</b>		H	0.60	6.9
<b>17b</b>		F	0.60	15
<b>18<sup>10</sup></b>		H	0.25	1.4
<b>15<sup>19</sup></b>		F	0.26	4.2
Razaxaban <sup>6a</sup>		F	0.19	2.1

$K_i$ s obtained from purified human enzymes and are averaged from multiple determinations ( $n = 2$ ). PT values are measured according to Ref. 6.

the binding and clotting assays than those with the substituent (i.e., **6a** vs **7a** and **6f** vs **7c**). The replacement of the 3- $CF_3$  with a 3- $CH_3$  substituent on the pyrazole scaffold was also investigated (Table 2). The compounds were less potent in the binding assay, but still showed sub-nanomolar inhibition and improved potency in the clotting assay.

The permeability Caco-2 assay, pharmacokinetics (determined in dogs), and in vivo antithrombotic efficacy (rabbit arterio-venous shunt thrombosis model) are shown in Table 3. The measured oral bioavailability ( $F$  %) was good in most cases. The pharmacokinetics and Caco-2 permeability values could in part explain

the oral bioavailability seen with these compounds. The pharmacokinetic profile for compounds **6a,d**, and **e** was comparable to that of razaxaban with moderate half life, whereas compounds **6f,g,h** and **7c** showed low clearance, low  $V_{dss}$ , moderate half life and high oral bioavailability. This is quite possibly due to the hydroxyl substituent on the cyclic amino moiety (the rationale for the improved pharmacokinetics due to the presence of the hydroxyl substituent on the P4 moiety is not understood). Although the 3-methylpyrazolo compounds **12a–d** were relatively potent in vitro, their pharmacokinetic profiles were moderate to poor. Overall compounds **6a, f, 7c**, and **12c** had the best in vitro potency and dog pharmacokinetic profiles.

**Table 2.** In vitro activity—biaryl P4 analogs

**6** R = H  
**7** R = F

**12a-c** R = H  
**12d** R = F

Compound	R <sup>1</sup>	fXa K <sub>i</sub> (nM)	Ha K <sub>i</sub> (nM)	PT IC <sub>2x</sub> (μM)
<b>6a</b>	NMe <sub>2</sub>	0.04	43	2.7
<b>6b</b>	NEt <sub>2</sub>	0.11	97	3.0
<b>6c</b>	N(Me)Et	<0.1	57	3.2
<b>6d</b>	NHMe	0.34	150	3.7
<b>6e</b>	Pyrrolidine	0.15	58	3.2
<b>6f</b>	3( <i>R</i> )-OH-pyrrolidine	0.03	35	3.6
<b>6g</b>	3( <i>S</i> )-OH-pyrrolidine	0.12	59	4.8
<b>6h</b>	4-OH-piperidine	0.22	71	4.9
<b>6i</b>	Morpholine	0.35	130	41
<b>6j</b>	4-NH-piperazine	0.64	280	14
<b>6k</b>	4-Me-piperazine	0.71	230	31
<b>7a</b>	NMe <sub>2</sub>	0.13	75	5.6
<b>7b</b>	Pyrrolidine	0.24	—	6.1
<b>7c</b>	3( <i>R</i> )-OH-pyrrolidine	0.16	72	8.4
<b>12a</b>	NMe <sub>2</sub>	0.55	380	2.1
<b>12b</b>	Pyrrolidine	0.31	120	1.4
<b>12c</b>	3( <i>R</i> )-OH-pyrrolidine	0.27	130	2.8
<b>12d</b>	3( <i>R</i> )-OH-pyrrolidine	0.34	250	4.9
Razaxaban <sup>6a</sup>	—	0.19	540	2.1

K<sub>i</sub>s obtained from purified human enzymes and are averaged from multiple determinations (*n* = 2). PT values are measured according to Ref. 6.

In the rabbit arteriovenous shunt (AVShunt) thrombosis model,<sup>5f</sup> the 3(R)-hydroxypyrrolidinyl compound **6f** was found to be the most potent compound from this series (IC<sub>50</sub> = 135 nM). The dimethylaminomethyl biaryl compound **6a** was about twofold less potent (IC<sub>50</sub> = 223 nM). The pyrazole compound **6f** was 97.4% protein bound (equilibrium dialysis assay).<sup>16</sup> In the same model, compounds **6h** and **7a–c** inhibited

thrombus formation with IC<sub>50</sub> values of 510, 600, 1000, and 600 nM, respectively. The high IC<sub>50</sub> values were in good agreement with the high clotting (PT) values. It is also possible that this could be attributed to the low plasma free fraction for these compounds (>98% plasma protein bound for **7a–c**).

The X-ray structure of compound **6f** (Fig. 3) bound in the active site of fXa shows a tight inhibitor enzyme complex<sup>17</sup> and follows the general trend seen with razaxaban. In the SI pocket, the aminobenzisoxazole PI group is in close proximity to Asp189 (2.8 Å). The 3-trifluoromethylpyrazole substituent engages the enzyme at the outer ridge of the SI region and is in close contact with the disulfide bridge. The pyrazole N-2 ring atom interacts with the NH backbone of Gln192 (3.3 Å). The carboxamido carbonyl oxygen of **6f** strongly interacts with the NH of Gly216 (3.0 Å) and positions the biaryl moiety in the S4 region in an optimal fashion. The terminal phenyl ring of the biphenyl forms an edge to face interaction with Try215, and is neatly π stacked between the Try99 and Phe174 residues. The 3-(R)-

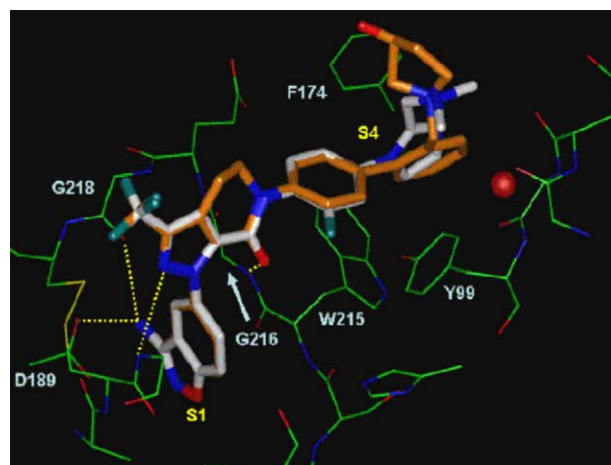


**Figure 3.** Overlap X-ray structures of BMS-740808 (**6f**, orange)<sup>20</sup> and razaxaban (white)<sup>6a</sup> in the active site of factor Xa.

**Table 3.** Permeability, pharmacokinetic, and in vivo antithrombotic profiles

Compound	Caco-2 <sup>a</sup> P <sub>app</sub> × 10 <sup>-6</sup> cm	Cl <sup>b</sup> (L/kg/h)	V <sub>dss</sub> <sup>d</sup> (L/kg)	t <sub>1/2</sub> <sup>d</sup> (po) (h)	F % <sup>d</sup> (po)	Rabbit <sup>c</sup> AVShunt IC <sub>50</sub> (nM)
<b>6a</b>	4.7	0.98	4.5	3.8	50	223
<b>6d</b>	—	1.66	9.7	7.4	67	—
<b>6e</b>	—	1.01	5.0	5.3	37	—
<b>6f</b> (BMS-740808)	1.7	0.35	1.6	5.1	82	135
<b>6g</b>	—	0.27	1.12	4.5	52	—
<b>6h</b>	0.4	0.21	1.4	6.4	102	510
<b>7a</b>	8.9	1.05	8.8	6.4	83	600
<b>7b</b>	bql	0.79	4.8	4.9	85	1000
<b>7c</b>	13.0	0.35	2.8	5.9	81	600
<b>12a</b>	6.8	3.2	6.4	1.6	13	—
<b>12b</b>	—	1.9	3.3	1.7	10	—
<b>12c</b>	6.2	0.42	0.75	1.7	44	<sup>d</sup>
<b>12d</b>	—	0.94	1.1	1.1	62	—
Razaxaban <sup>6a</sup>	5.56	1.1	3.4	5.3	84	340

<sup>a,b,c</sup> Caco-2, dog PK and rabbit AVShunt were measured according to Refs. 7a and b.

<sup>d</sup> ID<sub>50</sub> determined to be 0.6 μg/kg/h.



hydroxypyrrolidinomethyl moiety is within bonding distance with the electron-rich residues of the S4 region. Overall, these compounds fit into the fXa enzyme active site in a highly complementary manner.

To fully appreciate the binding affinity seen with **6f** a detailed kinetic study was conducted.<sup>11</sup> As expected for an active site-directed inhibitor, **6f** was competitive with a tripeptide chromogenic substrate, but exhibited mixed-type inhibition with the physiological substrate, prothrombin, where the binding interactions are predominantly at exosites.<sup>12</sup> Such substrate-dependent modes of inhibition were also observed with the Daiichi fXa inhibitor, DX-9065a.<sup>13</sup> There was no evidence for any significant binding of **6f** to the zymogen, fX. One consequence of this inhibition mechanism is that **6f** is a potent, low nanomolar, inhibitor in the presence or absence of saturating levels of the physiological substrate. The second order rate constant for association determined by stopped-flow spectrofluorimetry is rapid and near the diffusion controlled limit at both 25 °C and 37 °C ( $2.7 \times 10^7$  and  $1.8 \times 10^7$  M<sup>-1</sup> s<sup>-1</sup>, respectively). Similar rapid onset of inhibition has been reported for optimized thrombin inhibitors.<sup>14</sup> The plots of the observed rate constants versus inhibitor were linear up to 10 μM for **6f**, suggesting that binding occurs either by a simple one-step mechanism or by a two-step mechanism with very weak initial complex formation (initial  $K_i \gg 10$  μM). Differences in the dissociation rate constants calculated from the relationship,  $K_i = k_{\text{dissoc}}/k_{\text{assoc}}$ , account primarily for the higher  $K_i$  at 37 °C (0.00008 μM) and for the curved time courses observed at 25 °C (data not shown), which are often seen with slow, tight binding inhibitors ( $t_{1/2}$  off = 13 min at 25 °C and 8 min at 37 °C).<sup>15</sup> Similar results were obtained with razaxaban and will be reported elsewhere.<sup>11</sup> Table 4 shows the enzyme selectivity profile of **6f** compared to that of razaxaban. With the exception of thrombin, the compound is highly selective over a range of enzymes evaluated.

In conclusion, structural modification of the pyrazole scaffold resulted in the identification of a pyrazolopyridinone scaffold with excellent potency, selectivity, and favorable pharmacokinetics. Stability (pH) studies on **6f** showed no degradation of the molecule. Also, metabolic studies showed no cleavage of the carboxamido moiety. Overall, compound **6f** demonstrated excellent potency, desirable enzyme kinetic properties, and selectivity in vitro, good permeability, favorable pharmacokinetic and antithrombotic efficacy profile. The crystalline HCl salt of **6f** was selected for further pre-clinical evaluation as BMS-740808.

**Table 4.** Enzyme selectivity profile of **6f** (BMS-740808)

Human enzyme ( $K_i$ )	BMS-740808, <b>6f</b> , (μM)	Razaxaban (μM) <sup>6a</sup>
Factor Xa	0.00003	0.00019
Thrombin	0.035	0.540
Trypsin, plasma kallikrein, APC, factor IXa, factor VIIa, plasmin, Chymotrypsin, tPA	>2.8	>2.3

## Acknowledgment

The authors thank Dr. Steven Sheriff for depositing the BMS-740808/fXa complex into the PDB.

## References and notes

- (a) Hyers, T. M. *Arch. Intern. Med.* **2003**, *163*, 759; (b) Stein, P. D.; Grandison, D.; Hua, T. A. *Postgrad. Med. J.* **1994**, *70*(suppl 1), S72; (c) Hirsh, J.; Poller, L. *Arch. Intern. Med.* **1994**, *154*, 282.
- Weitz, J. I. N. *Engl. J. Med.* **1997**, *337*, 688.
- Turpie, A. G. G.; Antman, E. M. *Arch. Intern. Med.* **2001**, *161*, 1484.
- (a) Adang, A. E. P.; Rewinkel, J. B. M. *Drugs Future* **2000**, *25*, 369; (b) Rewinkel, J. B. M.; Adang, A. E. P. *Curr. Pharm. Des.* **1999**, *5*, 1043; (c) Samama, M. M.; Gerotzi-fas, G. T. *Thromb. Res.* **2003**, *109*, 1.
- (a) Walenga, J. M.; Jeske, W. P.; Hoppensteadt, D. *Curr. Opin. Investig. Drugs* **2003**, *4*(3), 272; (b) Samama, M. M. *Thromb. Res.* **2002**, *106*, V267; (c) Kaiser, B. *Cell. Mol. Life Sci.* **2002**, *59*, 189; (d) Leadley, R. J., Jr. *Curr. Top. Med. Chem.* **2001**, *1*, 151; (e) Hauptmann, J.; Stürzebecher, J. *Thromb. Res.* **1999**, *93*, 203; (f) Wong, P. C.; Crain, E. J.; Watson, C. A.; Zaspel, A. M.; Wright, M. R.; Lam, P. Y. S.; Pinto, D. J.; Wexler, R. R.; Knabb, R. M. *J. Pharmacol. Exp. Ther.* **2002**, *303*, 993; (g) Wong, P. C.; Pinto, D. J.; Knabb, R. M. *Cardiovasc. Drug Rev.* **2002**, *20*(2), 137; The race to an orally active fXa inhibitor. Recent advances (h) Quan, M. L.; Smallheer, J. *Curr. Opin. Drug Discovery Dev.* **2004**, *7*(4), 460.
- (a) Quan, M. L.; Lam, P. Y. S.; Han, Q.; Pinto, D. J.; He, M.; Li, R.; Ellis, C. D.; Clark, C. G.; Teleha, C. A.; Sun, J. H.; Alexander, R. S.; Bai, S. A.; Luetzgen, J. M.; Knabb, R. M.; Wong, P. C.; Wexler, R. R. *J. Med. Chem.* **2005**, *48*, 1729; (b) Lessen, M. R.; Davidson, B. L.; Gallus, A.; Pineo, G.; Ansell, J.; Deitchman, D. *Blood* **2003**, *102*, 15a, Abstract 41; (c) Wong P, Crain E, Quan M, Knabb R, Watson C, Staus A. ISTH XXth Congress, Sydney Australia, August 6–12, 2005.
- (a) Pinto, D. J. P.; Orwat, M. J.; Wang, S.; Fevig, J. M.; Quan, M. L.; Amparo, E.; Cacciola, J.; Rossi, K. A.; Alexander, R. S.; Smallwood, A. M.; Luetzgen, J. M.; Liang, L.; Aungst, B. J.; Wright, M. R.; Knabb, R. M.; Wong, P. C.; Wexler, R. R.; Lam, P. Y. S. *J. Med. Chem.* **2001**, *44*, 566; (b) Wong, P. C.; Quan, M. L.; Crain, E. J.; Watson, C. A.; Wexler, R. R.; Knabb, R. M. *J. Pharmacol. Exp. Ther.* **2000**, *292*, 351.
- Pruitt, J. R.; Pinto, D. J. P.; Galemno, R. A.; Alexander, R. S.; Rossi, K. A.; Wells, B. L.; Drummond, S.; Bostrom, L. L.; Burdick, D.; Bruckner, R.; Chen, H.; Smallwood, A.; Wong, P. C.; Wright, M. R.; Bai, S.; Luetzgen, J. M.; Knabb, R. M.; Lam, P. Y. S.; Wexler, R. R. *J. Med. Chem.* **2003**, *46*, 5298.
- Lam, P. Y. S.; Clark, C. G.; Li, R.; Pinto, D. J.; Orwat, M. J.; Galemno, R. A.; Fevig, J. M.; Teleha, C. A.; Alexander, R. A.; Smallwood, A. M.; Rossi, K. A.; Wright, M. R.; Bai, S. A.; He, K.; Luetzgen, J. M.; Wong, P. C.; Knabb, R. M.; Wexler, R. R. *J. Med. Chem.* **2003**, *46*, 4405.
- Fevig, J. M.; Cacciola, J.; Buriak, J., Jr.; Rossi, K. A.; Knabb, R. M.; Luetzgen, J. M.; Wong, P. C.; Bai, S. A.; Wexler, R. R.; Lam, P. Y. S. *Bioorg. Med. Chem. Lett.* **2006**, *16*, 3755.
- Experimental details for the mechanism studies are described in a manuscript in preparation on razaxaban.
- Krishnaswamy, S. *J. Thromb. Haemost.* **2004**, *3*, 54.
- Rezaie, A. R. *J. Thromb. Haemost.* **2003**, *89*, 112.

14. Elg, M.; Gustafsson, D.; Deinum, J. *J. Thromb. Haemost.* **1997**, 78, 1286.
15. Data were analyzed by standard methods established for slow binding inhibitors Kettner, C.; Mersinger, L.; Knabb, R. *J. Biol Chem.* **1990**, 265, 18289.
16. Pacific, G. M.; Viani *Clin. Pharmacokinet* **1992**, 23, 449.
17. The X-ray structure of **6f** bound to human fXa was obtained at 2.2 Å resolution with a crystallographic *R*-value of 0.260 (*R*-free of 0.296) with a 1 $\sigma$  cutoff according to the methodology described in Ref. 7.
18. (a) Ioannides, C.; Lewis, D. F. V.; Trinick, J.; Neville, S.; Sertkaya, N. N.; Kajbaf, M.; Gorrod, J. W. *Carcinogenesis* **1989**, 10, 1403; (b) Chung, K. T.; Chen, S.-C.; Wong, T. Y.; Li, Y.-S.; Wei, C.-L.; Chou, M. W. *Toxicol. Sci.* **2000**, 56, 351.
19. Quan, M. L.; Han, Qi.; Fevig, J.; Lam, P. Y. S.; Bai, S.; Knabb, R. M.; Luetttgen, J. M.; Wong, P. C.; Wexler, R. R. *Bioorg. Med. Chem. Lett.* **2006**, 16, 1795–1798.
20. Coordinates and structure amplitudes for **6f** have been deposited in the PDB with accession no. 2FZZ.